

# NIGHTTIME VENTILATION BY STACK EFFECT

J. van der Maas, Ph.D.

C.-A. Roulet, Ph.D.

## ABSTRACT

*In the summer, ventilation at night is used to increase thermal comfort in an experimental three-level laboratory. To this effect, special apertures, which stay open during the summer nights, are provided at ground level and on the roof, allowing natural ventilation of the high-mass staircase and building. This paper concerns a case where the high-mass staircase (all internal doors closed) was cooled by stack ventilation. The temperatures of the inflowing air, the exhaust air, and the wall were measured as a function of time. The time dependence of the exhaust air and wall temperatures is compared with a simple dynamic model that couples air flow, heat transfer, and a thermal model for the wall. The agreement is good. The heat loss rate is an output parameter that can be used in energy calculations. For given openings, the model predicts that the total heat extracted from the building during the night can be maximized by increasing the heat-exchanging surface area (e.g., all internal doors open) and by increasing the thermal effusivity,  $\sqrt{\lambda \rho c}$ , of the wall materials. Further validation of the model is needed and mechanical ventilation should be included. However, in principle, a simple design tool can be made showing the effect of opening sizes, wall surface area, and wall thermal properties on the energy consequences of night ventilation for a particular climate.*

## INTRODUCTION

The exchange of indoor air with fresh outdoor air can provide cooling if the latter is at a lower temperature than the indoor air. A situation where this convective cooling is a practical proposition arises when the internal heat gain or solar heat gain through windows would raise the indoor temperature even higher than the outdoor air temperature.

Convective cooling is very useful in heavy buildings located in climates where large diurnal temperature variations occur. To improve indoor thermal conditions, structures of large thermal capacity are used to reduce the indoor temperature swing. The indoor temperature then tends to be close to the average outdoor temperature, and nighttime ventilation can be effective in reducing the average indoor air temperature (Koenigsberger et al. 1973).

In the handbooks, architects are told to provide for burglar- and mosquito-proof openings that should be large enough to ensure adequate night ventilation (Koenigsberger et al. 1973; ASHRAE 1989). However, as far as the authors know, a design tool allowing the dimensioning of natural-ventilation openings is not readily available.

As the basis of a design tool, energy calculations of ventilative cooling must be performed. However, with the heat removal capacity of a given flow rate of ventilating air being proportional to the temperature difference between supply and exhaust air, the key issue becomes the evaluation of the exhaust air temperature (Antinucci et al. 1989). Another difficult issue is the estimate of the volume flow rate itself, which depends, for example, on internal flow resistances.

Jacobus van der Maas is a Research Physicist and Claude-Alain Roulet is a Research Group Leader with LESO-PB (Solar Energy and Building Physics Laboratory of the EPFL (Ecole Polytechnique Fédérale de Lausanne, Swiss Federal Institute of Technology), Lausanne, Switzerland.

The event that led to the work reported here is the successful use of ventilative night cooling in an experimental three-level building that is instrumented and can be monitored while in use. Over the years, it was found that thermal comfort during the summer increased with night ventilation. However, architects asking how to achieve optimal performance could not be answered satisfactorily. Indeed, while special burglarproof ventilation apertures are provided at ground level and on the roof, the dimensioning of the apertures was not based on calculation but on the feeling of the architect that the available areas (two 0.5 m<sup>2</sup> [5.4 ft<sup>2</sup>] openings) would do the job.

Therefore, having found that a simple algorithm correctly predicts the ventilative cooling rate after the opening of a door or window in an otherwise closed room (van der Maas et al. 1989, 1990), it was decided to test the validity range of this model further and start measurements on the whole building.

This algorithm links stack ventilation to heat transfer and a wall thermal model and predicts the influence of building materials and opening sizes on the heat transferred out of the building by ventilative cooling. The assumptions of the present formulation are:

1. The airflow rate is calculated from the stack equation using a single discharge coefficient for the inlet and exhaust openings. A situation where the airflow is concentrated in the wide staircase of the building is a good approximation.
2. Wind or mechanical ventilation is not included. This is not an intrinsic limitation of the model, requiring only a modification of the airflow part of the model.
3. The indoor air temperature is taken to be homogeneous and equal to the exhaust air temperature. While a vertical temperature stratification in the staircase is always observed, this simplification implies that the indoor-outdoor temperature difference should be large with respect to the indoor temperature variation with height.
4. The walls, characterized by a single parameter, are thick (not necessarily of high mass) and in thermal equilibrium with the building when ventilation starts.

Finally, actual measurements have shown that the model correctly predicts stack ventilation for the staircase, providing heat loss rates as a function of time and requiring few input parameters. Therefore, this model can be used for simple energy calculations of stack ventilative night cooling, showing the influence of ventilation opening dimensions, building materials, and climate.

## ALGORITHM FOR VENTILATIVE COOLING

For a given flow rate, the heat-removal capacity of ventilating air is proportional to the temperature difference

between supply and exhaust air, and the key issue is to evaluate the temperature of the exhaust air. Once the exhaust air temperature is known, the volume flow rate can be easily calculated from the stack velocity and the opening sizes, provided one knows the internal flow resistances. The stack velocity varies as the square root of the product  $H\Delta T$ , where  $H$  is the vertical distance between the inlet and exhaust openings, and  $\Delta T$  is the temperature difference between the inlet and exhaust temperatures. If there is a single space between the inlet and exhaust openings (e.g., a staircase), the flow resistance is given by the discharge coefficients of the openings. The latter coefficients can be determined by comparing the air velocity measurements with the stack velocity equation.

The proposed ventilation model follows naturally from observations made on the temperatures in a volume in thermal equilibrium with the surrounding building structure. After starting ventilation with cold outside air, one first observes a sudden drop in the exhaust air temperature, followed by a slow decrease with time. Because the wall surface temperature is systematically higher than the inside air temperature, heat transfer takes place from the wall to the air. It appears that the initial temperature drop is larger when reducing the wall surface area or increasing the ventilation rate, and a heat transfer coefficient can be defined. Further, one notes that the slow decrease in exhaust air temperature is due to an overall decrease in wall surface temperature. The latter is found by solving the heat equation.

Finally, the new model couples the ventilative heat loss rate with the heat transfer between the air and the walls and a decreasing wall surface temperature. The ventilation and thermal models form a four-node network that will be discussed in the following sections (see Figure 1). Two new parameters are introduced—the heat-exchanging wall surface area and the thermal effusivity of the wall material.

### Ventilation Model

Consider a volume (e.g., a staircase) with an outlet on the top (opening area  $A_{out}$ ), an inlet a distance  $H$  below (opening area  $A_{in}$ ), and an inside/outside temperature difference,  $T_{in} - T_{out}$ . Then the expressions for the stack velocity in the exhaust ( $v_{out}$ ), the volume flow rate ( $\dot{V}$ ), and the ventilation heat loss rate ( $\Phi_v$ ) are given by

$$v_{out} = C_1 \sqrt{2g \left( \frac{T_{in} - T_{out}}{T} \right)} \quad (1)$$

$$\sqrt{1 + (A_{out}/A_{in})^2},$$

$$\dot{V} = A_{out} \cdot v_{out} \quad (2)$$

and

$$\Phi_v = C_p \rho \dot{V} (T_{in} - T_{out}) \quad (3)$$

The exhaust velocity (Equation 1) follows from the Bernoulli equation and the ideal gas law (ASHRAE 1985), assuming a single discharge coefficient ( $C_1$ ).  $T$  (in Kelvin) is the average absolute temperature of the inside and outside temperatures. It is assumed that there is a single neutral pressure level that is situated between the two openings.

This implies that the opening heights should be much smaller than the distance between the middle of the two openings,  $H$ , and that  $A_{in}$  and  $A_{out}$  are of the same order of magnitude. Finally, it is expected that the discharge coefficient ( $C_1$ ) is about 0.6, the typical value for sharp-edged orifices. In Figure 1, the ventilation model is represented by thermal resistance number one, its value being given by Equation 3.

### Thermal Model

The basic assumption of the following approach is that before starting the ventilation, the building is in quasi-thermal equilibrium, and only perturbations from this equilibrium situation are considered without having to know the steady-state energy balance of the enclosure. One of the consequences of initial thermal equilibrium is the neglect of radiation. Radiant heat transfer remains inside the ventilated volume, thermally coupling the walls together, thereby influencing at most the internal thermal stratification (Sandberg 1990). Some radiant heat loss through the ventilation openings takes place, but this is neglected.

**Heat Balance** The mean air temperature follows from the heat balance inside a volume with a ventilative heat loss rate,  $\Phi_v$ , and convective heat transfer to the internal room surface,  $S_i$  (Figure 1):

$$C_m \frac{dT_m}{dt} = -\Phi_v + h_c S_i (T_{wall} - T_m) \quad (4)$$

where  $C_m$  is a heat capacity and  $h_c$  is a mean convective heat transfer coefficient.  $C_m$  includes both the heated air volume and the (empirical) effect of furnishings.

**Heat Transfer Coefficient** It is assumed that the internal walls of the enclosure are homogeneous or that at least average wall properties can be defined. The heat load is transmitted to the walls by convection through a thermal boundary layer resistance. It was found that the use of an average heat transfer coefficient with a value typical of low-velocity forced convection,  $h_c = (6 \pm 1) \text{ W/m}^2 \cdot \text{K}$  [(1.1 ± 0.2)

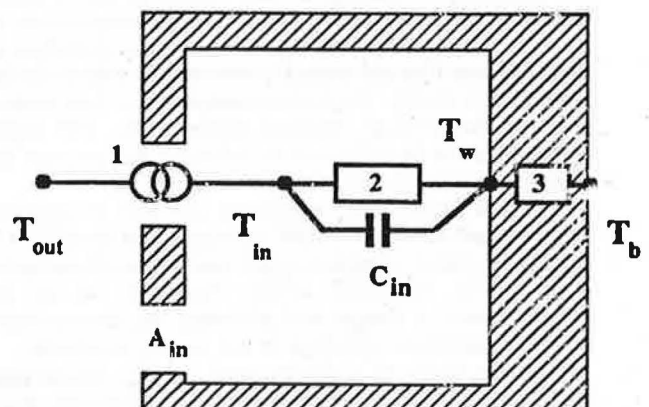


**Figure 1** The coupled ventilation and thermal models represented by a four-node network. (1) Ventilative heat loss (Equation 3) modeled as a current source between inside and outside temperature. (2) Boundary layer resistance (Equation 7) shunted by an empirical heat capacity  $C_m$ . (3) The dynamic thermal resistance of the wall (Equation 9).  $T_b$  is  $T_{wall}$  ( $t = 0$ ), the wall temperature when heat flow starts.

Btu/h-ft<sup>2</sup>-°F], gives consistent results. The thermal resistance between the air and the walls then equals  $1/S_i h_c$  K/W (h-°F/Btu), where  $S_i$  is the total wall surface area. This resistance can be measured independently by measuring the wall and air temperatures for a known heat flow rate.

For a cooling rate ( $\Phi_v$ ) of the ventilated space, and neglecting the heat capacity  $C_m$ , the average density of the heat flow rate is  $q = \Phi_v/S_i$ , and the difference between the wall surface temperature,  $T_{wall}$ , and the air temperature,  $T_a$ , is

$$T_{wall} - T_a = q/h_c = \Phi_v/(S_i h_c) \quad (5)$$

**Time Constant** Before the ventilation starts,  $q = 0$  and  $T_a = T_{wall}$ . As was discussed by van der Maas et al. (1989) and Yaneske and Forrest (1978), when cooling begins at  $t = 0$ , the first term in the heat balance (Equation 4) cannot be neglected and the air-wall temperature difference ( $T_{wall} - T_a$ ) rises nearly exponentially to the limiting value,  $\Phi_v/(S_i h_c)$ :

$$T_{wall} - T_a = (1 - \exp(-t/\tau)) \Phi_v/(S_i h_c) \quad (6)$$

From the heat balance (Equation 4), a single time constant,  $\tau = C_m/h_c S_i$ , can be defined when  $\Phi_v$  is a constant. The calculated value for  $\tau$  is typically a few minutes for air (unfurnished rooms), and this effect can be neglected for long ( $t \gg \tau$ ) time periods.

**Coefficient  $C_2$**  For cases where the exhaust opening is not situated at the top of the ventilated volume, only the wall surface below the upper level of the opening will receive the full cooling load. Temperature stratification will result, and the walls above the opening will stay relatively warm (the upper space will cool, however, by radiation to the lower space). In order to be able to quantify this effect,  $S_i$  is substituted by  $C_2 S_i$ , where the coefficient  $C_2$  gives the fraction of the total wall surface area that is active in the heat transfer process. From Equation 6, the inside air temperature becomes

$$T_a(t) = T_{wall}(t) - (1 - \exp(-t/\tau)) \Phi_v/(C_2 S_i h_c) \quad (7)$$

For the studied staircase,  $C_2$  is close to unity. Note that the temperature stratification as characterized by  $C_2$  is situated above the ventilated space and should not be confused with temperature stratification between the ventilation openings. The heat transfer resistance (2) in Figure 1 follows from Equation 7.

**Wall Thermal Model** In studying the transient thermal behavior of the ventilated space, one is interested in the time dependence of the surface temperature of the wall,  $T_{wall}$ , submitted to a boundary condition of heat flow rate density,  $q$ .

The solution of the heat equation for this situation can be found in Carslaw and Jaeger (1959) and is for a semi-infinite solid:

$$T_{wall}(t) - T_{wall}(0) = \frac{1}{b\sqrt{\pi}} \int_0^t q(t-\tau) \tau^{-1/2} d\tau \quad (8)$$

where  $b = \sqrt{\rho c \lambda}$  (the square root of the product of thermal conductivity, density, and specific heat) is the

thermal effusivity of the wall material (ISO 1987). For a constant value of  $q$ , Equation 8 simplifies to

$$\begin{aligned} T_{wall}(t) - T_{wall}(0) \\ = \Delta T_{wall}(t) = \frac{2q}{b} \sqrt{\frac{t}{\pi}} = R_{dyn} q \end{aligned} \quad (9)$$

where  $R_{dyn}$  is the dynamic thermal resistance per wall surface area, which is zero at time  $t = 0$  and increases with the square root of time. In the present model, the simpler expression (Equation 9) is used even when  $q$  does vary with time. This approximation means that the real time history of  $q$  is replaced with a history of constant  $q$ . This appears to be an acceptable approximation, particularly when  $q$  varies slowly with time. As an example, one can calculate the wall temperature for the case where consecutively (1)  $q = \text{constant}$ , (2) a stepfunction for a certain time is applied, and (3)  $q = \text{constant}$  again. A comparison of the solutions of Equations 8 and 9 shows that the memory of the applied stepfunction fades out in about as much time as the step lasted, and the solution of Equation 8 goes asymptotically to the solution for constant  $q$  (Equation 9).

In Figure 1, number 3 is the thermal wall resistance (Equation 9) situated between the wall surface temperature,  $T_w = T_{wall}(t)$ , and the building temperature,  $T_b = T_{wall}(0)$ .

**Thin Walls** For long time periods, even thick walls cannot be considered semi-infinite, and a thermal wall model more detailed than Equation 8 should be used. The high-mass floors and walls of the laboratory did not show a noticeable departure from the behavior predicted by Equation 9 for up to 10 hours (van der Maas 1989, 1990), and the model is sufficiently accurate for tests lasting up to one night. In case the model is used for situations where walls should be considered thin, the wall surface temperature and the exhaust air temperature are overestimated and, therefore, the cooling rate as well.

**Thermal Effusivity ( $b$ )** The material property  $b = \sqrt{\rho c \lambda}$  (the square root of the product of thermal conductivity, density, and specific heat [ISO 1987]) is relevant to the nonsteady state, and, among others, the thermal effusivity,  $b$ , accounts for the response of a surface temperature to a change of the heat flow density at the surface. The lower the thermal effusivity of the material, the more sensitive the surface temperature is to changes of heat flow at the surface.

When the walls of the enclosure are homogeneous, there is no difficulty in finding a theoretical value for the wall thermal effusivity,  $b$ . However, this becomes difficult for composite walls or for situations where the various wall surfaces are of a different nature or heterogeneous. For these situations, it is advantageous to use a simple experimental technique to measure an apparent  $b$  (van der Maas 1989, 1990; Yaneske and Forrest 1978). Indeed, for a known heat flux density, a plot of the wall temperature as a function of the square root of heating time is linear (Equation 9) and  $b$  can be determined experimentally from the slope of such a plot.

### Solution of the Algorithm

As illustrated by Figure 1, the ventilative heat loss is found by solving the nonlinear set of Equations 3, 7, and 9 simultaneously. By varying  $T_{in}$ , a solution is found for every value of  $t$  in a few iterations. Once  $T_{in}$  is known, the heat loss rate is calculated from Equation 3.



## EXPERIMENTAL TECHNIQUES

### Building Description

A high-mass solar energy laboratory has offices at ground level and at the first and second levels. The central staircase extends to the cellar (level -1) and to the roof (level 3). The staircase is ventilated at night by burglarproof openings at the entrance ( $1.04 \text{ m}^2$  [ $11 \text{ ft}^2$ ] effective ventilation area) and by the open roof door ( $1.78 \text{ m}^2$  [ $19 \text{ ft}^2$ ]). The staircase walls are made of masonry and the floors and flat roof of massive concrete. A large portion of the internal separation (south) wall surface is made up of wooden doors. All the other walls, the floor, and the ceiling have 20 cm [ $0.7 \text{ ft}$ ] of glass wool insulation as a second layer. While the thermal properties of each surface element are well known, there is considerable uncertainty in a calculated average value of the thermal effusivity characteristic for the whole staircase. Calculated and experimental values of the thermal effusivity (van der Maas et al. 1989, 1990) were consistent with a value of  $b = 1,000 \text{ J}/(\text{m}^2 \cdot \text{K} \cdot \text{s}^{0.5})$  ( $100 \text{ Btu}/(\text{ft}^2 \cdot ^\circ\text{F} \cdot \text{h}^{0.5})$ ), with an uncertainty of 20%.

The total wall surface area of the staircase (volume 4.5 by 8 by 15 =  $540 \text{ m}^3$  [ $15 \text{ by } 26 \text{ by } 49 = 19,000 \text{ ft}^3$ ]) is calculated to be  $700 \text{ m}^2$  ( $7,500 \text{ ft}^2$ ) with a 10% uncertainty. The massive (20 to 30 cm [ $1 \text{ ft}$ ] thick) concrete staircase itself is exposed on both sides and constitutes about 50% of the total heat-exchanging surface area. It is worth mentioning that the staircase is in contact with the vertical walls at only a few places, so that vertical airflow along the walls is possible.

### Measurement Methods

The temperatures of the inflowing air, the exhaust air, and the wall, as well as the exhaust air velocity, were measured as a function of time. The exhaust air temperature and velocity were measured with a flow analyzer system. The temperature transducer is a  $50\text{-}\mu\text{m}$ -diameter thermistor. The absolute accuracy of the temperature measurements is  $\pm 0.5 \text{ K}$  (at air velocities  $> 5 \text{ cm/s}$  [ $0.16 \text{ ft/s}$ ]), with a time constant of less than 1 second. The velocity sensor is a calibrated, omnidirectional, constant-temperature anemometer with a time constant of less than 0.1 second. Its measuring accuracy is 2.5% of the reading, and the influence of the air temperature is less than  $0.2\%/\text{K}$ . The temperature of the inflowing air was measured with a thermocouple device (reproducibility  $0.2 \text{ K}$ , accuracy  $\pm 0.5 \text{ K}$ ), with the thermocouple being placed in the airstream.

Wall temperatures were scanned with a radiation infrared thermometer. Using the built-in black cell for calibration, measurements were reproducible within  $0.5 \text{ K}$ . The radiation thermometer was used mainly for the detection of local changes in surface temperature. The measured temperatures were checked against thermocouple readings. During ventilation, inside air temperatures were measured with a thermocouple device at  $50 \text{ cm}$  ( $1.5 \text{ ft}$ ) normal to the position where the wall temperature was measured.

## EXPERIMENTAL RESULTS

### Test of the Ventilation Model

The stack equation (Equation 1) has been tested by measuring the exhaust velocity for various temperature differences and for various magnitudes of  $A_{in}$  and  $A_{out}$ . The discharge coefficient should then be evaluated from these

tests. However, the velocity was found to vary by about 50% over the exhaust opening. By averaging the velocities over the opening, the volume flow rate was estimated with about 15% uncertainty, being consistent with Equation 1 and a discharge coefficient of  $0.65 \pm 0.1$ . In previous work (van der Maas 1989, 1990), a discharge coefficient of 0.6 was used for lack of reliable data. In the following, and for reasons of consistency, the same value of  $C_1 = 0.6$  will be used.

### Tests of the Thermal Model

**Heat Transfer with Fan Heater** The thermal model was first tested separately from the ventilation model by heating the unvented enclosure with fan heaters. Fan heaters have the advantage that the air is made slightly turbulent and the convective heat transfer coefficient is about  $6 \text{ W}/\text{m}^2 \cdot \text{K}$  ( $1.1 \text{ Btu}/\text{h} \cdot \text{ft}^2 \cdot ^\circ\text{F}$ ), which is typical for low-velocity forced convection (Yaneske and Forrest 1978; van der Maas et al. 1990). The ventilative heat loss rate ( $-\dot{\Phi}_v$ ) in Equation 4 is then replaced by a convective heat source pumping heat into the air at  $T_a$  at a constant rate ( $+\dot{\Phi}$ ), and one expects a constant temperature difference to develop between the walls and the inside air. This temperature difference should agree with Equation 7 and allows one to check the consistency of the parameter values  $b$ ,  $S_p$ , and  $h_c$ .

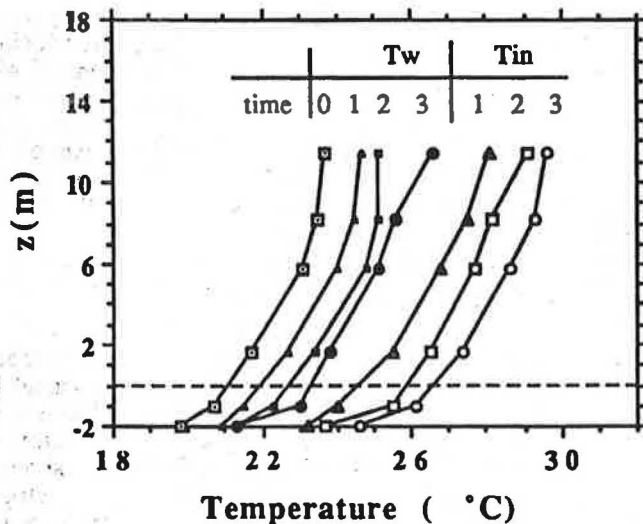
Before the heater experiment, the nonvented building was monitored for 24 hours to determine the importance of building temperature drift. While the outside temperature varied between  $8^\circ\text{C}$  ( $46^\circ\text{F}$ ) and  $25^\circ\text{C}$  ( $77^\circ\text{F}$ ), the inside air temperature variation was only  $2 \text{ K}$ . In the following, no correction for building drift has been made.

The staircase (calculated total surface area  $S_p = 700 \text{ m}^2$  [ $7,500 \text{ ft}^2$ ]) was heated by a series of electric fan heaters distributed equally over the various levels. The total electrical power was  $\dot{\Phi} = 13 \text{ kW}$  ( $13 \text{ Btu/s}$ ), giving an average heat flux density of about  $18 \text{ W}/\text{m}^2$  ( $5.7 \text{ Btu}/\text{h} \cdot \text{ft}^2$ ).

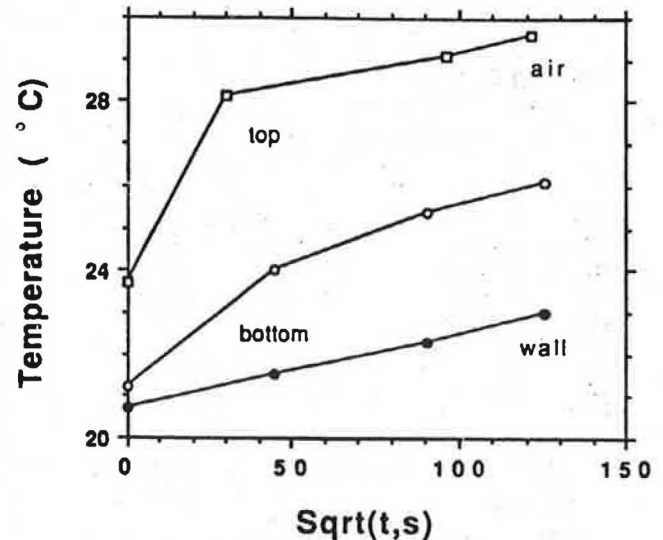
Figure 2a gives the wall and air temperatures as a function of height from ground level before heating started and after about 0.5, 2, and 4 hours of heating. The vertical temperature gradients of the wall and the air appear to be nearly equal and constant in time, and the difference  $T_w - T_a = 3 \text{ K}$  is consistent with  $h_c = (6 \pm 1) \text{ W}/\text{m}^2 \cdot \text{K}$  ( $1.1 \text{ Btu}/\text{h} \cdot \text{ft}^2 \cdot ^\circ\text{F}$ ), confirming previous measurements.

Figure 2b is a plot of air and wall temperatures as a square root of heating time. It follows from Equations 7 and 9 that the slope of such a plot should be constant for  $t > \tau$  and equal to  $1.13 (\dot{\Phi}/S_p b)$ . From these data,  $b = 1,000 \text{ J}/(\text{m}^2 \cdot \text{K} \cdot \text{s}^{0.5})$  [ $100 \text{ Btu}/(\text{ft}^2 \cdot ^\circ\text{F} \cdot \text{h}^{0.5})$ ] is found with 10% precision.

**Heat Transfer during Night Ventilation** Wall and air temperatures were measured in the staircase as a function of height during night ventilation. In Figure 3a the temperature stratification of the inside air is shown when the ventilation has just started (19 h) and 4 and 10 hours later. At ground level ( $z = 0$ ), the cool air enters the building. The wall temperature gradient remains almost constant during cooling (Figure 3b). It is noted that the cool air fills the cellar level of the staircase ( $z = -2 \text{ m}$  [ $-6 \text{ ft}$ ]) and provides similar cooling there as for the higher levels. The wall air temperature difference (Figure 3c) is a measure of the local heat flux density ( $h_c$  assumed constant). When ventilation starts, the inflowing outside air is  $19^\circ\text{C}$  and slightly warmer than the temperature in the cellar. Initially, the air wall temperature difference (and, therefore, the cooling rate) is smallest near the ground level and increases with height. But the air wall temperature difference appears



**Figure 2a** The staircase ( $S_i = 700 \text{ m}^2$  [7,500  $\text{ft}^2$ ]) heated with  $\Phi = 13 \text{ kW}$  (13 Btu/s) electrical power (all the internal and external doors were closed). Electrical fan heaters are distributed over the various building levels. The wall and air temperatures are plotted as a function of height (ground level  $z = 0$ , dashes) at time 0 and after about 0.5, 2, and 4 hours heating time: 1, 2, 3.  $T_{in} - T_w \approx 3 \text{ K}$  is consistent with  $6 \pm 1 \text{ W/m}^2 \cdot \text{K}$  (1.1 Btu/h·ft $^2$ ·°F).



**Figure 2b** The air (open symbols) and wall temperature plotted as a function of the square root of heating time. Both at the top ( $z = 11.5 \text{ m}$ ) and at the bottom ( $z = -1 \text{ m}$ ) of the staircase, the temperature variation is similar. From Equations 7 and 9 ( $t \gg \tau$ ), the slope is  $dT/d\sqrt{t} = 1.13 (\Phi/S_i b)$ , resulting in the experimental value  $b = (1 \pm 0.1) \times 10^3 \text{ J/(m}^2 \cdot \text{K} \cdot \text{s}^{0.5})$  [100 Btu/(ft $^2$ ·°F·h $^{0.5}$ )].

to become constant almost independently from height (Figure 3c). Using the (calculated) ventilative heat losses (see also Figure 6), a single heat transfer coefficient of  $(5.5 \pm 0.8) \text{ W/m}^2 \cdot \text{K}$  (1 Btu/h·ft $^2$ ·°F) is found to be consistent with these data, which is 10% lower than the value used in the model calculations.

### Stack Ventilative Cooling

The measured exhaust temperature during night cooling was compared with the model predictions for three different cases (see Figures 4 through 6). The following parameter values were used in the simulation:  $C_1 = 0.6$ ,  $C_2 = 1$ ,  $h_c = 6 \text{ W/m}^2 \cdot \text{K}$  (1.1 Btu/h·ft $^2$ ·°F),  $H = 9.6 \text{ m}$  (32 ft),  $A_{in} = 1.04$  or  $1.98 \text{ m}^2$  (11 or 21 ft $^2$ ),  $A_{out} = 1.78 \text{ m}^2$  (19 ft $^2$ ), and  $S_i = 700 \text{ m}^2$  (7,500 ft $^2$ ). The time constant is three minutes and the wall is characterized by  $b = 1,000 \text{ J/(m}^2 \cdot \text{K} \cdot \text{s}^{0.5})$  [100 Btu/(ft $^2$ ·°F·h $^{0.5}$ )]. For the simulations a linear outside temperature variation was used, which, in Figures 5 and 6, is given together with the measured outside temperature.

The wall temperature at  $t = 0$  was taken to be equal to the exhaust air temperature at  $t = 0$ . This is an acceptable approximation as long as the vertical temperature variation in the building is small compared to the inside-outside temperature difference.

**Case 1** The results and analysis for the first case are given in Figures 4a, b, and c. During the two-hour ventilation period, the entrance door was open ( $A_{in} = 1.98 \text{ m}^2$  [21 ft $^2$ ]) and the outside temperature stayed constant,  $T_{out} = (9.5 \pm 0.5)^\circ\text{C}$  [49°F]. Ventilation started at  $t = 0$ , and in Figure 4a are plotted the measured and calculated exhaust air temperatures (open circles and drawn curve) and the calculated wall temperature.

The influence on exhaust temperature of opening the inside doors from the staircase to the offices (at initial

building temperature) was checked during ventilation. First, the doors were opened at all levels (marked 1 in Figure 4a); then, at 10-minute intervals, the inner doors were closed subsequently on the ground floor, the second floor, and the first floor. Assuming that the opening of internal doors is equivalent to increasing the heat-exchanging surface area,

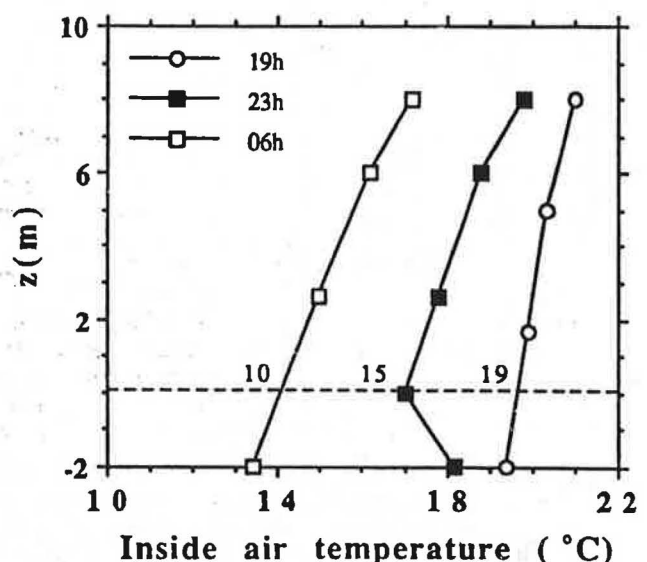


**Figure 3a** Air temperature stratification in the staircase measured at three moments (7 p.m., 11 p.m., and 6 a.m.) during night ventilation. Ventilation started at 6.30 p.m. The air inlet temperatures (19°C, 15°C, and 10°C; ground level, dashed) are given.

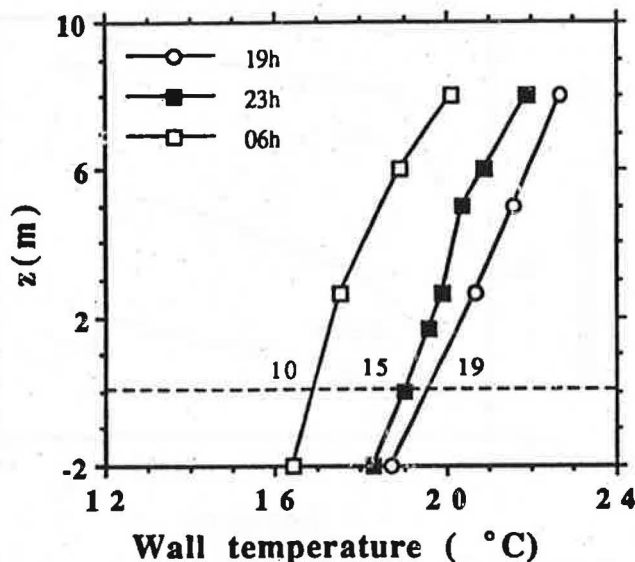


**Figure 3b** Wall temperature stratification in the staircase measured at three moments (7 p.m., 11 p.m., and 6 a.m.) during night ventilation (compare Figure 3a).

$S_i$  (about 500 m<sup>2</sup> [5,400 ft<sup>2</sup>] per floor), the resulting exhaust air temperatures can be roughly understood (Figure 4b).

When the ventilation opening is closed after two hours (Figure 4a), the measured exhaust air temperature rises rapidly to the wall temperature at the roof level with the same time constant as when the ventilation started, and the rise in temperature during the next two hours closely resembles the form of the initial two-hour cooling curve.

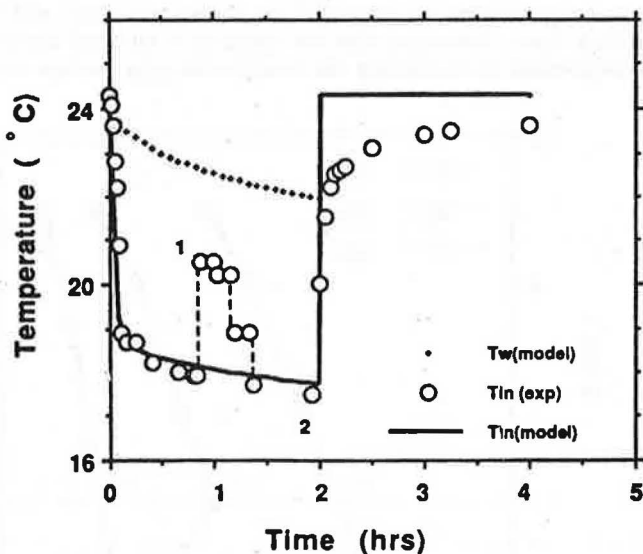


**Figure 4a** Case 1. The measured,  $T_{in}(exp)$ , and predicted,  $T_{in}(model)$ , outlet air temperatures and the calculated wall temperature ( $T_w$ ) as a function of ventilation time.  $A_{in} = 1.98 \text{ m}^2$  (21 ft<sup>2</sup>).  $A_{out} = 1.78 \text{ m}^2$  (19 ft<sup>2</sup>).  $H = 9.6 \text{ m}$  (30 ft).  $T_{out} = 9.5 \pm 0.5^\circ\text{C}$  (49°F). Ventilation starts at  $t = 0$ , stops at  $t = 2 \text{ h}$ . All doors opened at all levels (marked 1); at 10-minute intervals, inner doors closed subsequently on the ground floor, the second floor, and the first floor.

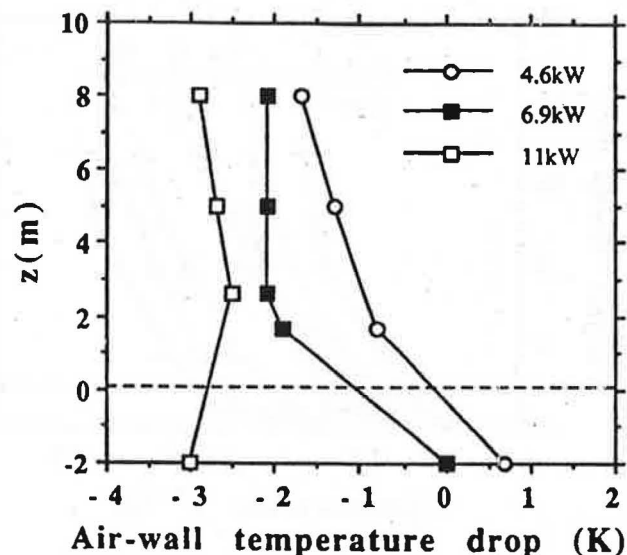


**Figure 3c** Air-wall temperature differences as a function of height at three moments (7 p.m., 11 p.m., and 6 a.m.) during night ventilation (compare Figures 3a, 3b). The ventilative heat loss rates are calculated by the model (see Figure 6). The data are consistent with a heat transfer coefficient of  $5.5 \pm 0.8 \text{ W/m}^2\cdot\text{K}$  ( $0.55 \pm 0.1 \text{ Btu/h}\cdot\text{ft}^2\cdot^\circ\text{F}$ ).

The details of this behavior could be reconstructed with the help of Equations 4 and 8 but not with Equations 7 and 9 used in the simplified model. Indeed, when cooling stops, the model predicts  $T_{wall}$  to jump back to the initial temperature at  $t = 0$ , while in reality it relaxes back slowly as shown.

Figures 4b and 4c show the influence of the heat-exchanging surface area,  $S_i$ , on the inside air temperature and the cooling power, showing that of the potential cooling power of nearly 40 kW, less than 50% is used by ventilating the staircase alone.

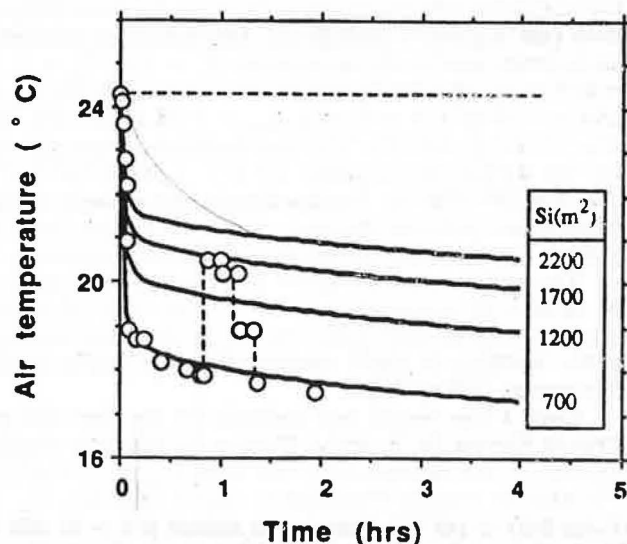


**Figure 4b** Case 1. Measured  $T_{in}$  compared with exhaust air temperatures calculated for four different values of the heat-exchanging surface area  $S_i$  (compare Figure 4a).  $T_{in}(t = 0)$ , dashed.



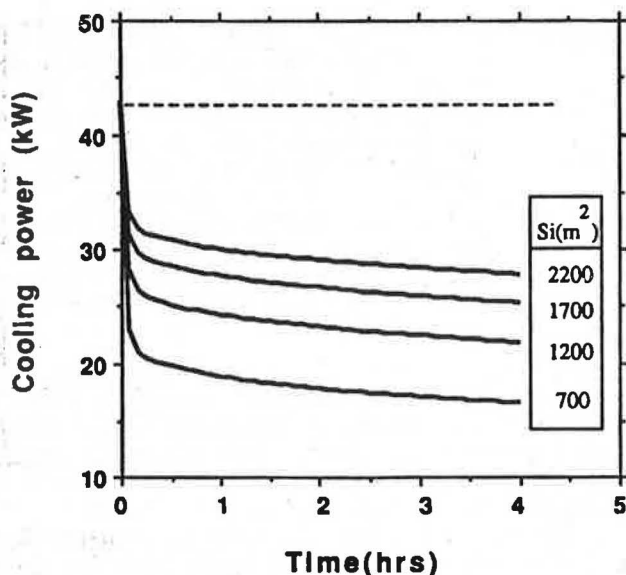


Figure 4c Case 1. The cooling power for four different values of the heat-exchanging surface area  $S_i$  (compare Figure 4b).  $\Phi(t=0)$ , dashed.

Case 2 Figure 5 shows an example of night ventilation lasting from about 10 p.m. to 8 a.m. The inlet area is  $A_{in} = 1.04 \text{ m}^2$  (11 ft<sup>2</sup>). The outdoor temperature was lowest at 6:30 a.m. The calculated exhaust air temperature,  $T_{ex}$ , is about one degree too low, which is nearly 10% of  $T_{in} - T_{out}$ , and  $\Phi$  is therefore underestimated by up to 15%, showing the kind of precision we can expect from such a simplified model. Because in this case both the inside and outside temperatures decrease, both the ventilative heat loss rate,  $\Phi$ , and the temperature difference,  $T_{wall} - T_{in}$ , tend to be constant, so that Equation 9 is a good approximation. The model also predicts correctly a decreased heat loss in the morning due to the increase in outdoor temperature. The total calculated energy loss (10 hours) is 90 kWh, which is underestimated by about 15%.

Case 3 Figure 6 shows an example of night ventilation that started at 6.30 p.m. on a sunny day. In contrast to the results given in Figure 5, the measured exhaust temperature (open circles) is much lower than predicted by the model, although the form of the curves is very similar. Indeed, the initial wall temperature used in the calculation (by assumption equal to the exhaust air temperature at  $t=0$ ) appears to be too high and not representative for the staircase. Indeed, the assumption that the vertical temperature variation in the building is small compared to the inside-outside temperature difference is not valid here, and, to be correct, the temperature stratification should be included in the model.

The air and wall temperatures reported in Figures 3a and 3b refer to this data series. From Figure 3c it is clear that at 7 p.m., the air-wall temperatures at the ground and first level are small, and that the heat transfer is concentrated in the upper half of the staircase. Because the model implicitly assumes that heat transfer is equally distributed over the wall surface area, the calculated exhaust air temperature is higher than the measured air temperature. By the end of the ventilation period, the experimental air-wall temperature drop (Figure 3c, 6 a.m.) is nearly independent of height and comes close to the calculated value (Figure 6). The total calculated energy loss (10 hours) is 56 kWh, which is overestimated by 10% to 20%.

## DISCUSSION

To show the relative importance of wall area and material choice, we have made a case study and calculated the total energy loss (10 hours) for a number of values of  $S_i$ ,  $b$ , and initial inside-outside temperature difference,  $T_{in} - T_{out}$ . The results are plotted in Figure 7. Thick curves correspond to a heavy building structure and the thinner lines to a lightweight structure with four times lower thermal effusivity walls. New experiments are planned in order to test the three elements of the model (airflow, heat transfer, and wall thermal model) on their validity range.

The airflow model can be improved by including internal flow resistances, mechanical ventilation, and wind; special opening configurations can be studied with particular discharge coefficients and flow interactions; and the temperature stratification in the ventilated space (see Figure 3) can be included. The heat transfer model can be made more detailed, and the wall thermal model can be extended to include special cases.

What did not come out of the presented results is the importance of the parameter  $C_2$ . As shown for the case of single-sided ventilation (van der Maas et al. 1989, 1990), this parameter can vary considerably; for example, when the exhaust is not on the roof, but at the second level, then  $C_2 \approx 0.7$ .

On the other hand, this model suggests that inlet openings could be provided at the first level instead of at ground level, reducing stratification below the air inlet and

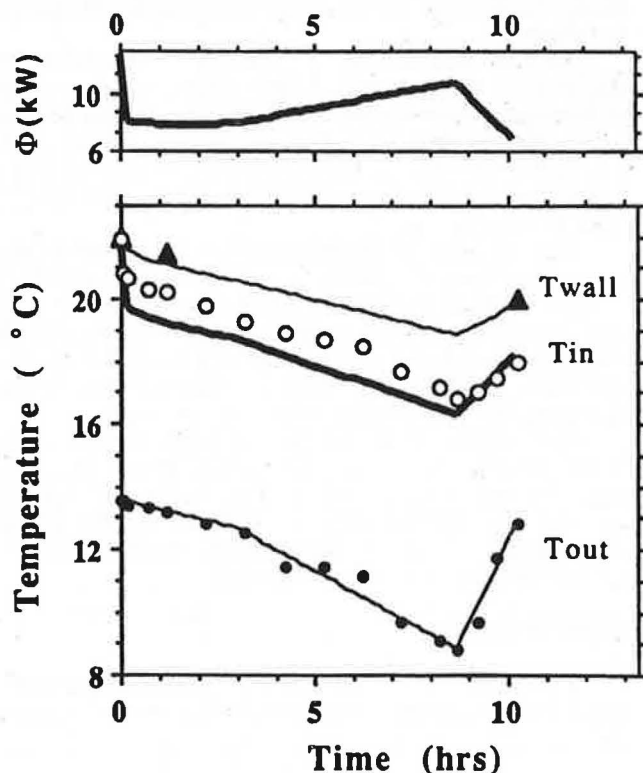
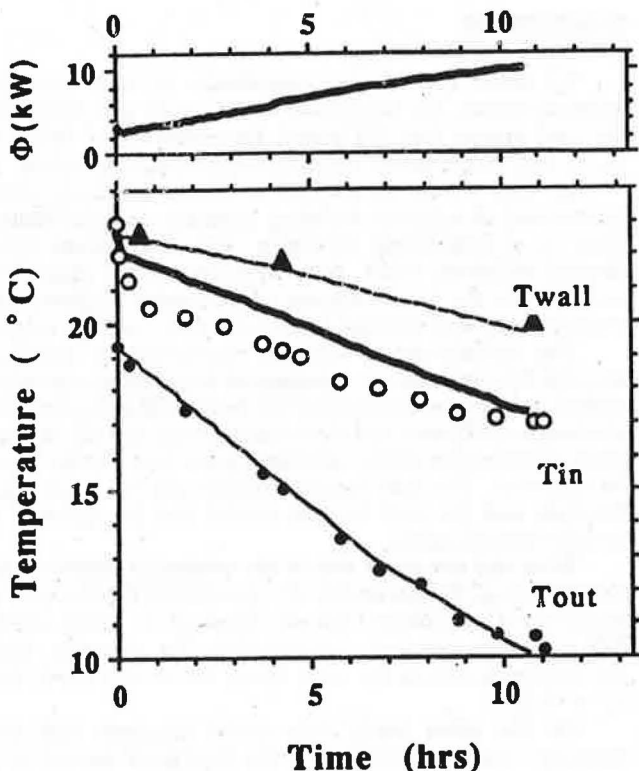


Figure 5 Case 2. Night ventilation from about 10 p.m. to 8 a.m. The measured and calculated exhaust air temperature,  $T_{ex}$ , the outside temperature,  $T_{out}$ , the wall temperature,  $T_{wall}$ , and the calculated heat loss rate,  $\Phi$ , as a function of ventilation time.  $A_{in} = 1.04 \text{ m}^2$  (11 ft<sup>2</sup>).  $A_{out} = 1.78 \text{ m}^2$  (19 ft<sup>2</sup>).  $H = 9.6 \text{ m}$  (30 ft). The calculated energy loss (10 h) is 90 kWh.



**Figure 6** Case 3. Night ventilation from about 6.30 p.m. to 6 a.m. The measured and calculated exhaust air temperature,  $T_{\text{ex}}$ , the outside temperature,  $T_{\text{out}}$ , the wall temperature,  $T_{\text{wall}}$ , and the calculated heat loss rate,  $\Phi$ , as a function of ventilation time.  $A_{\text{in}} = 1.04 \text{ m}^2$  (11  $\text{ft}^2$ ).  $A_{\text{out}} = 1.78 \text{ m}^2$  (19  $\text{ft}^2$ ).  $H = 9.6 \text{ m}$  (30 ft). The calculated energy loss (10 h) is 56 kWh. The air and wall temperatures as a function of height are given at 7 p.m., 11 p.m., and 6 a.m. in Figures 3a and 3b.

easing the problem for the architect of making the openings burglarproof.

As mentioned before, the staircase is in contact with the vertical walls at only a few places, so that vertical airflow along the walls is possible and continuous boundary layers can be formed. Smoke flow visualizations during ventilation have shown that the boundary layer is turbulent, which explains the relatively high value for the boundary layer resistance.

The wall thermal model used here is limited to situations where the wall can be considered semi-infinite and is in quasi-thermal equilibrium when ventilation starts. This means that the time scale of the cooling should be relatively short. For the present study, the limit is reached after about one night. To treat longer time periods or thinner walls, a more detailed wall thermal model can be used.

This simple model for passive night cooling clearly shows the interaction of the main parameters of the opening sizes, heat-exchanging surface area, inside wall material, and climate. By providing an estimate of the possible energy loss by stack ventilation, it can be used to develop a simplified design tool for architects.

## CONCLUSIONS

This paper concerns a model for passive night cooling tested on the high-mass staircase of a three-level laboratory

cooled by stack ventilation. The time dependence of the exhaust air and wall temperatures is correctly explained by a simple dynamic model that couples airflow, heat transfer, and a thermal model for the wall without the need for adjusting coefficients. The heat loss rate is an output parameter that can be used in energy calculations.

The temperature stratification in the staircase is not taken into account, which means that the inside air temperature variation with height is assumed to be small with respect to the indoor-outdoor temperature difference.

The heat transfer between the air and the walls is taken to be uniform over the total surface area of the staircase, with an overall heat transfer coefficient of  $6 \text{ W/m}^2\cdot\text{K}$  (1  $\text{Btu/h}\cdot\text{ft}^2\cdot^\circ\text{F}$ ).

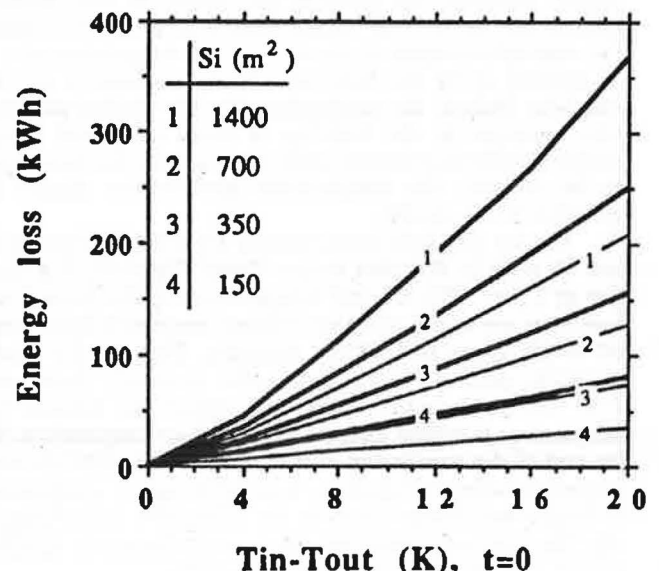
The wall thermal model, assuming semi-infinite walls (characterized by an average value for the thermal effusivity of  $b = \sqrt{\lambda\rho c}$ ), requires thermal equilibrium when ventilation starts and is valid for one night. The model can be extended to take into account internal building resistances, wind, and mechanical ventilation.

Finally, the model can be implemented in a simple design tool for the evaluation of the effect of opening sizes, wall surface area, and wall thermal properties on the energy consequences of night ventilation for a particular climate.

## ACKNOWLEDGMENTS

This research was sponsored by the Swiss Federal Energy Office (OFEN). We are most grateful to Dr. Alfred Moser (ETHZ, Zurich) and to Dr. Bernard Fleury (LASH, Lyon, France) for comments and helpful discussions.

**Figure 7** Simulation of energy loss by nighttime ventilation. Calculated is the total energy loss integrated over 10 hours as a function of  $S_i$ ,  $b$ , and initial inside-outside temperature difference,  $T_{\text{in}} - T_{\text{out}}$  ( $t = 0$ );  $T_{\text{out}} = \text{constant}$ .  $b = 1,000$  (thick curve) and  $250$  (thin curve)  $\text{J}/(\text{m}^2\cdot\text{K}\cdot\text{s}^{0.5})$  [ $100 \text{ Btu}/(\text{ft}^2\cdot^\circ\text{F}\cdot\text{h}^{0.5})$ ].  $A_{\text{in}} = 2 \text{ m}^2$  (20  $\text{ft}^2$ ).  $A_{\text{out}} = 2 \text{ m}^2$  (20  $\text{ft}^2$ ).  $H = 10 \text{ m}$  (33 ft).





## NOMENCLATURE

$a$	= thermal diffusivity, $\text{m}^2/\text{s}$
$A_{in}$	= inlet opening area, $\text{m}^2$
$A_{ex}$	= exhaust opening area, $\text{m}^2$
$b$	= thermal effusivity, $(\lambda \rho c)^{0.5} [\text{J}/(\text{m}^2 \cdot \text{K} \cdot \text{s}^{0.5})]$
$c$	= wall specific heat, $\text{J}/\text{kg} \cdot \text{K}$
$C_{in}$	= heat capacity inside air, $\text{J}/\text{K}$
$C_p$	= specific heat of air at constant pressure, $\text{J}/\text{kg} \cdot \text{K}$
$C_1$	= flow discharge coefficient
$C_2$	= wall surface fraction for heat transfer
$g$	= gravitational acceleration, $\text{m}/\text{s}^2$
$h_c$	= convective heat transfer coefficient, $\text{W}/\text{m}^2 \cdot \text{K}$
$H$	= distance between middle of inlet and exhaust apertures, $\text{m}$
$q$	= density of heat flow rate, $\text{W}/\text{m}^2$
$q_s$	= wall surface area, $\text{m}^2$
$t$	= time, $\text{s}$
$\bar{t}$	= mean absolute air temperature, $\text{K}$
$T_{in}$	= inside air temperature, $^{\circ}\text{C}$
$T_w, T_{ms}$	= wall surface temperature, $^{\circ}\text{C}$
$T_{out}$	= outside air temperature, $^{\circ}\text{C}$
$v$	= velocity, $\text{m}/\text{s}$
$\dot{V}$	= volume flow rate, $\text{m}^3/\text{s}$
$z$	= height in aperture, $\text{m}$
$\Phi_v$	= ventilation heat flow rate, $\text{W}$
$\lambda, k$	= thermal conductivity, $\text{W}/\text{m} \cdot \text{K}$
$\rho$	= density, $\text{kg}/\text{m}^3$

## REFERENCES

- Abrams, D.W. 1986. *Low energy cooling, A guide to the practical application of passive cooling and cooling energy conservation measures*. New York: Van Nostrand Reinhold.
- Antinucci, M., B. Fleury, J. Lopez d'Asiain, E. Maldonado, M. Santamouris, A. Tombazis, and S. Yannas. 1989. "Horizontal study on passive cooling for buildings." First draft. Brussels: Commission of the European Communities, Building 2000.
- ASHRAE. 1985. *ASHRAE handbook—1985 fundamentals*. Atlanta: American Society of Heating, Refrigerating, and Air-Conditioning Engineers, Inc.
- ASHRAE. 1989. *ASHRAE handbook—1989 fundamentals*. Atlanta: American Society of Heating, Refrigerating, and Air-Conditioning Engineers, Inc.
- Boutet, T.S. 1987. *Controlling air movement, A manual for architects and builders*. New York: McGraw-Hill.
- Carslaw, H.S., and J.C. Jaeger. 1959. *Conduction of heat in solids*, 2d ed. London: Oxford University Press.
- Heiselberg, P., and M. Sandberg. 1990. "Convection from a slender cylinder in a ventilated room." B2, 34, 20 pp., ROOMVENT '90, Oslo, June.
- ISO. 1987. Standard 7345, "Thermal insulation—physical quantities and definitions." Geneva: International Standards Organization.
- Koenigsberger, O.H., T.G. Ingersoll, A. Mayhew, and S.V. Szokolay. 1973. *Manual of tropical housing and building. Part one: Climatic design*. London: Longman Ltd.
- Liddament, M. 1986. "Air infiltration calculation techniques AIVC." Warwick, UK: Air Infiltration and Ventilation Center.
- Martin, M.F., B. Fleury, R. Kammerud, and T. Webster. 1984. "Parasitic power requirements for night ventilated nonresidential buildings." Solar Energy Program LBL, August 15, Contract No. DE-AC03-76SF00098.
- van der Maas, J., C.-A. Roulet, and J.-A. Hertig. 1989. "Some aspects of gravity driven air flow through large apertures in buildings." *ASHRAE Transactions*, Vol. 95, Part 2, pp. 573-583.
- van der Maas, J., C.-A. Roulet, and J.-A. Hertig. 1990. "Transient single sided ventilation through large openings in buildings." C48, ROOMVENT '90, Oslo, June.
- Yaneske, P.P., and I.D. Forrest. 1978. "The thermal response of rooms with intermittent, forced convective heating." *Building Services Engineer*, Vol. 46, pp. 13-17.

